Journal of Alloys and Compounds 581 (2013) 86–90

Contents lists available at SciVerse ScienceDirect

Journal of Alloys and Compounds

journal homepage: www.elsevier.com/locate/jalcom

Structural modifications in a $Mn_{54}Al_{43}C_3$ melt-spun alloy induced by mechanical milling and subsequent annealing investigated by atom probe tomography

J.M. Le Breton [a,*], J. Bran [a], E. Folcke [a], M. Lucis [b], R. Lardé [a], M. Jean [a], J.E. Shield [b]

[a] Groupe de Physique des Matériaux, UMR 6634 CNRS, Université et INSA de Rouen, 76801 Saint Etienne du Rouvray, France
[b] Department of Mechanical & Materials Engineering and Center for Materials and Nanoscience, University of Nebraska Lincoln, United States

ARTICLE INFO

Article history:
Received 12 March 2013
Received in revised form 28 June 2013
Accepted 1 July 2013
Available online 9 July 2013

Keywords:
Nanostructured intermetallics
Microalloying
Mechanical alloying and milling

ABSTRACT

The structural changes upon milling and subsequent annealing of a $Mn_{54}Al_{43}C_3$ alloy containing the intermetallic tetragonal $L1_0$ MnAl phase (τ phase) as the major phase were investigated by X-ray diffraction and atom probe tomography. The analyses show that milling the starting powder for 10 h leads to the nanostructuration of the sample. The milled sample is partly oxidised and contains both non oxidised $Mn_{60\pm5}Al_{40\pm5}$ regions and oxidised regions. Annealing the powder for 1 h at 500 °C leads to enrichment in Al of the oxidised regions, and to the phase transformation of the non-oxidised regions into a nanostructured β-Mn-like phase with a composition close to Mn_3Al_2.

1. Introduction

Mn–Al–C-based permanent magnets are nowadays of renewed interest as they are free from rare-earth elements. Their reasonably good intrinsic magnetic properties are due to the presence of the intermetallic tetragonal $L1_0$ MnAl phase (τ phase), which possesses strong uniaxial magnetic anisotropy [1]. The τ phase is obtained from the high temperature hcp ε phase [2–4], which is antiferromagnetic at temperatures lower than 97 K [5]. However, annealing the ε phase at temperatures below the eutectoid temperature for prolonged times leads to the formation of the equilibrium γ_2 and β phases [6].

The τ phase is metastable, and is stabilized by the addition of C to the Mn–Al alloy [7]. It has been shown that, in melt spun Mn–Al–C alloys the τ phase stabilized by C addition can be transformed reversibly into the ε phase at around 800 °C, without decomposition into the stable γ_2 and β phases [8], and Mn–Al–C permanent magnets can be obtained by melt spinning with subsequent annealing [8]. Mn–Al–C alloys containing the τ phase as the major phase can also be obtained after mechanical milling with subsequent annealing [9–11]. The magnetic properties of the annealed alloy are strongly dependent both on the fraction of the τ phase and its microstructure [9,11].

With the aim of obtaining nanostructured Mn–Al–C permanent magnets, with increased magnetic properties, we applied mechanical milling to melt-spun Mn–Al–C annealed alloys containing the τ phase. In this paper, we present the results of an investigation of the influence of both milling and subsequent annealing treatments on the structure of a Mn–Al–C alloy. The investigation has been carried down to the nanometer scale by atom probe tomography.

2. Experimental

$Mn_{54}Al_{43}C_3$ alloys were obtained by arc melting at 1200 °C of high purity elements. As-prepared ingots were melt-spun, and subsequently annealed for 1 h at 500 °C. These annealed ribbons were submitted to high energy ball milling in a SPEX 8000 mixer/mill for times up to 10 h under Ar atmosphere, and subsequently annealed for 1 h at 500 °C under Ar atmosphere.

Three samples were investigated: a melt-spun and annealed ribbon (so-called unmilled sample), a powder milled for 10 h (so-called milled sample), and a subsequently annealed powder (so-called annealed sample). For the analyses, the ribbon has been hand crushed in a mortar, and the resulting powder particles were investigated.

The X-ray Diffraction analyses were performed on a D8 Diffractometer (Bruker AXS), using Co Kα radiations ($\lambda_{K\alpha1}$ = 0.178897 nm and $\lambda_{K\alpha2}$ = 0.179285 nm). The software EVA was used to determine the different phases present in our samples with the help of the JCPDS database.

The Atom Probe Tomography (APT) experiments were performed with a Laser Assisted Wide Angle Tomographic Atom Probe (LAWATAP) from CAMECA. For such analyses, a single powder particle with a diameter ranged in 1–20 μm is mounted on a stainless steel fine tip needle with conductive epoxy glue using an ex-situ micro-manipulator and tip-shaped using a focused ion beam (FIB). FIB milling were performed using a dual beam Zeiss 1530 equipped with a GEMINI electron column and an Orsay physics ion (Ga) column. To prevent the region of interest from damages induced by high energy (30 keV) Ga implantation, the tip was finally cleaned up at low energy (2 keV). For more details, the tip preparation method is described elsewhere [12]. The atom probe analyses were then performed at 80 K in an ultra-

* Corresponding author. Tel.: +33 2 32 95 50 39; fax: +32 2 32 95 50 32.
E-mail address: Jean-Marie.LeBreton@univ-rouen.fr (J.M. Le Breton).

0925-8388/$ - see front matter © 2013 Elsevier B.V. All rights reserved.
http://dx.doi.org/10.1016/j.jallcom.2013.07.002

high vacuum chamber at a pressure of 10^{-9} mbar. The femtosecond laser pulse system used was an amplified ytterbium-doped laser (AMPLITUDE SYSTEM s-pulse) with a 350 fs pulse length and a 342 nm wavelength.

3. Results and discussion

3.1. X-ray diffraction

The XRD patterns of the unmilled, milled and annealed samples are shown in Fig. 1. In the pattern of the unmilled sample (Fig. 1a), sharp and intense peaks can be observed, which were indexed to the τ phase. The measured lattice parameters of the tetragonal τ phase ($a = 0.2761 \pm 0.0035$ nm and $c = 0.35970 \pm 0.0029$ nm) are in agreement with those taken from the JCPDS files 037–1073 and 048–1831 for $Mn_{53.7}Al_{43.6}C_{2.7}$ ($a = 0.27685$ nm and $c = 0.35995$ nm, s.g. P4/mmm) and $Mn_{54.5}Al_{42.0}C_{3.5}$ ($a = 0.2759$ nm and $c = 0.3598$ nm, s.g. P4/mmm) respectively. This shows that the metastable $L1_0$ MnAl phase is the main constituent of the unmilled sample. Peaks with a weak intensity corresponding to the γ_2 (Al_8Mn_5) phase were also observed. The measured lattice parameter of the cubic γ_2 phase ($a = 0.9023 \pm 0.0081$ nm) is in agreement with the JCPDS file 049–1279 ($a = 0.9012$ nm, s.g. I-43m). The weak intensity of the corresponding peaks indicates the presence of the γ_2 phase as a minor phase in the unmilled sample. At this stage, the τ phase is obtained as the major phase in the sample but the small width of the corresponding peaks indicates that the grains are not nanostructured. After 10 h of milling, broad and low intense peaks are observed in the corresponding XRD pattern (Fig. 1b). This could indicate the presence of a disordered MnAl phase with a reduced grain size. In the pattern of the annealed sample (Fig. 1c), sharp and intense peaks are observed, which correspond to a well crystallized β-Mn-like phase. It is worth noticing that, compared with a pure β-Mn phase, these peaks are shifted to lower angles, in agreement with the presence of Al atoms in the phase. The measured lattice parameter of the cubic β-Mn-like phase ($a = 0.64260 \pm 0.0041$ nm) is closer to that of Mn_3Al_2 ($a = 0.6411$ nm, s.g. P4132) than to that of β-Mn ($a = 0.63245$ nm, s.g. P4132). This result indicates that 10 h milling and subsequent annealing lead to the transformation of the metastable τ phase in a β-Mn(Al) phase, with a composition close to Mn_3Al_2.

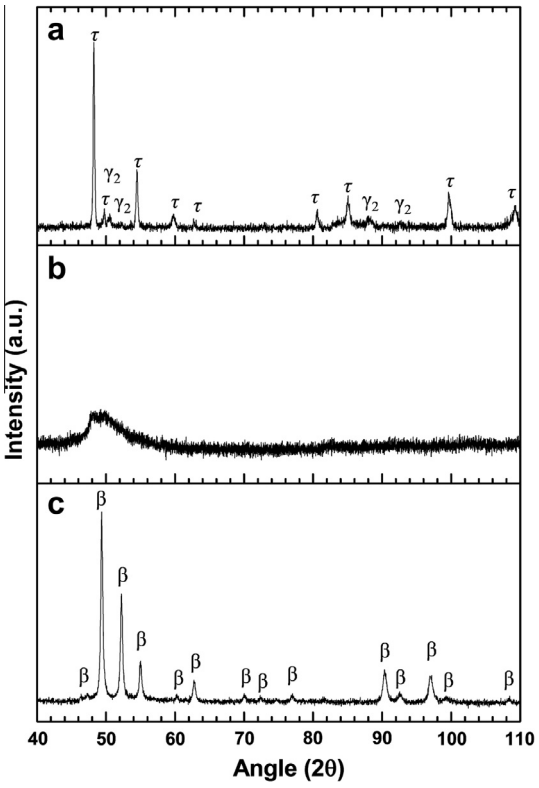

Fig. 1. XRD patterns of the unmilled (a), 10 h milled (b) and 10 h milled and annealed (c) samples: τ = $L1_0$ MnAl phase $\gamma_2 = Al_8Mn_5$ phase β = β-Mn(Al) phase.

3.2. Atom probe tomography

With the aim of investigating the nanostructure of the powders down to the nanometer scale, Atom Probe Tomography was used. The mass spectra given by this technique represent the number of evaporated species in function of their mass-over-charge ratio. The mass spectra of the three samples are shown in Fig. 2. It can be

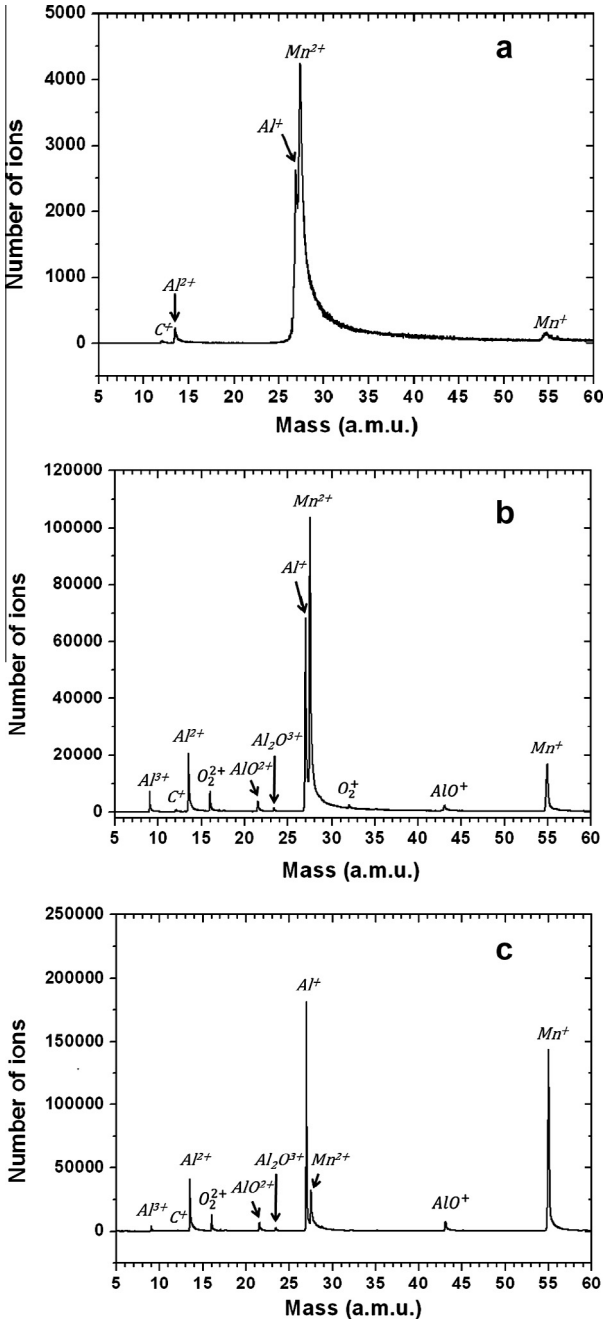

Fig. 2. APT mass spectra of the unmilled (a), milled (b) and annealed (c) samples.